https://doi.org/10.5194/hess-2020-96
Preprint. Discussion started: 14 May 2020

Hydrology and Earth System Sciences
Discussions

3D Multiple-point Statistics Simulations of the Roussillon Continental Pliocene Aquifer using DeeSse

Valentin Dall'Alba[1], Philippe Renard[1], Julien Straubhaar[1], Benoit Issautier[2], Cédric Duvail[3], and Yvan Caballero[2]

[1]Center of Hydrogeology and Geothermics (CHYN), University of Neuchâtel. Rue Emilie Argand 11 CH-2000, Neuchâtel, Switzerland
[2]French Geological Survey (BRGM)
[3]GEOTER SAS, FUGRO Group

Correspondence: Valentin Dall'Alba (valentin.dallalba-arnau@unine.ch)

Abstract. This study presents a novel workflow to model the internal heterogeneity of complex aquifers using the multiple-point statistics algorithm DeeSse. We illustrate the applicability of this workflow on the Roussillon's aquifer in the region of Perpignan (southern France). This work is part of a project aiming at assessing the groundwater dynamics of this Mediterranean aquifer in the context of a growing population, climate change, and increasing pressure on the freshwater resources. We focus here on the geological heterogeneity of the Continental Pliocene layer because it is expected to influence possible saltwater intrusion process and its corresponding uncertainty quantification. The main aim of the paper is therefore to describe the procedure that is used to model the aquifer heterogeneity with a relatively small number of direct geological observations and a well defined geological concept. When few direct observations are available, the traditional geostatistical approaches cannot be applied easily because variogram inference is difficult. On the opposite, multiple-point statistics simulations can rely on a conceptual geological model. Here, the conceptual model consists not only of a training image displaying the spatial organization of the main sedimentological elements in space, but also in a set of additional information such as general trends and paleo orientations of the sedimentological features. The direct sampling algorithm DeeSse can be used in this context to model the expected heterogeneity. The workflow involves creating 2D non-stationary training images (TI) coupled during simulation with auxiliary information and controlled by hard conditioning data obtained from interpreted electrofacies. To control the non-stationarity, a 3D trend map is obtained by solving numerically the diffusivity equation as a proxy to describe the spatial evolution of the sedimentary patterns, from the source of the sediments to the outlet of the system. A 3D continuous rotation map is estimated from paleo orientations of the fluvial system. Both trend and orientation maps are derived from geological insights gathered from outcrops and general knowledge of processes occurring in these types of sedimentary environments. Finally, the 3D model is obtained by stacking 2D simulations following the paleo-topography of the aquifer. The vertical facies transition between two 2D simulations is controlled by both the hard conditioning data set and by simulating conditional data points from one simulation to another. This process allows to bypass the creation of a 3D training image while preserving the vertical continuity of the sedimentary objects.

https://doi.org/10.5194/hess-2020-96
Preprint. Discussion started: 14 May 2020

Hydrology and Earth System Sciences
Discussions

1 Introduction

It has been shown for example by Naranjo-Fernández et al. (2018) that accounting for heterogeneity is an important step in producing realistic hydrogeological models and to properly manage the water resource, especially in a context of global climatic changes. The present study proposes a new multivariate workflow, using a multiple-point statistics (MPS) approach, to model the spatial heterogeneity of complex alluvial aquifers. The workflow is applied to the Roussillon aquifer, which is a multi-layered system composed of the Marine Pliocene aquifer (PMS), the Continental Pliocene aquifer (PC), and the Quaternary aquifer (QT). Located along the southernmost part of the French Mediterranean coast, near the Spanish border, this system is used intensively both for drinkable water and irrigation (Aunay et al., 2006). From its social and economic importance, understanding the aquifer is essential for the authorities to ensure a long term and sustainable management of the resource. Since one of the largest source of uncertainty is the identification of the hydraulic conductivity field, it has been decided to first focus on the modeling of the complex geological heterogeneity of the Continental Pliocene layer. This layer consists of alluvial deposits and presents a high level of internal heterogeneity.

To model the heterogeneity, different geostatistical methods have been developed and used in the last decades (de Marsily et al., 2005). They were employed in different fields going from risk assessment, resources management, mining or petroleum engineering (Matheron, 1963; Strebelle et al., 2002; de Carvalho et al., 2017). All these methods aim to model the variables of interest at locations where they have not been measured. Traditional geostatistical methods are based on a covariance or variogram models inferred from the data. Kriging (Matheron, 1963) provides the best linear unbiased estimator, it is fast, and produces a smooth interpolation. Multi-Gaussian simulation methods, such as SGS proposed by Journel (1974)), are able to generate random fields, depicting the spatial variability of the variable of interest. Truncated Gaussian simulation methods (TGS or PGS) allow to generate discrete realizations where the spatial relation between the facies (categories) are derived from one or several underlying multi-Gaussian random fields (Matheron et al., 1987). However, these methods are based on two-point statistics and cannot reproduce some geological features such as the sinuosity of a channel or realistic sedimentological patterns. Hence, they are not always suitable for modelling the expected heterogeneities in geological reservoirs. Multiple-point statistics (MPS) has been developed since the 90's to overcome these limitations. MPS techniques allow to generate random fields reproducing the spatial statistics given in a training image (TI), which is a conceptual model that integrates the geological knowledge of the area of interest. Moreover, unlike traditional approaches, MPS does not require to define an analytical model to describe the spatial distribution of the modelled variable, instead it infers it in an implicit way from the TI provided by the user (Hu and Chugunova, 2008).

Many MPS algorithms have been developed over the years. The general principle consists in sequentially populating the simulation grid while reproducing the patterns (spatial statistics) present in the TI. For example, in SNESIM (Strebelle et al., 2002), the statistics of patterns on a pre-defined geometry are stored in a tree shape database that is built by scanning the whole TI before starting the simulation. Then, the simulation proceeds pixel by pixel, a value is drawn randomly according to probabilities conditioned by the surrounding patterns and computed from the data base. As a consequence, the method is memory consuming and limited to the simulation of categorical variables. In IMPALA (Straubhaar et al., 2011, 2013), the

https://doi.org/10.5194/hess-2020-96
Preprint. Discussion started: 14 May 2020


Hydrology and Earth System Sciences
Discussions

limitation due to the memory is alleviated by using a list shape database, and non-stationary TIs can also be handled with the use of auxiliary variables (Chugunova and Hu (2008)). In other algorithms, such as FILTERSIM (Zhang et al., 2006) or CCSIM (Tahmasebi et al., 2012), the simulation grid is filled by directly pasting patches, *i.e.* several pixels at a time. FILTERSIM allows the simulation of continuous variables, whereas CCISM is based on cross-correlation between patches. The main drawbacks of patch-based methods is their difficulty to honour conditioning data.

One of the most flexible MPS algorithms is the Direct Sampling (Mariethoz et al., 2010). It is a pixel-based method, where the simulation of one pixel consists in randomly searching for a pattern in the TI that is similar to the pattern centered on the considered pixel in the simulation grid, and then copying the value of the variable from the TI. Hence, it has the advantage of making database creation unnecessary, no probability is computed, and patterns of varying geometry are handled. By adapting the way of comparing the patterns in the TI and in the simulation grid, the algorithm is able to deal with categorical and continuous variables, as well as with the joint simulation of multiple variables. In this work, we use the direct sampling algorithm implemented in the DeeSse code (Straubhaar, 2019), It is parallelized and offers many options to constrain the simulation such as continuous rotation/affinity maps or proportion targets.

But to model an aquifer at a regional scale, a very important aspect is to account for all the non-stationarities due to the geological process such as the location of the sources of the sediments, their transport, and so on. The application of MPS to a real case, requires more than just an efficient MPS code and a good training image. It requires also to develop a methodology and a workflow to account for all those aspects.

The aim of this paper is therefore to introduce such a global workflow allowing to incorporate most of the available geological knowledge into a plausible heterogeneity model and to illustrate the method on the Roussillon plain. The workflow is generic and can be applied to any other case where the available data are scarce compared to the geological knowledge. The paper is structured as follows. The section 2 introduces some background information regarding the geology and hydrogeology of the Roussillon aquifer, followed by additional information on the DeeSse algorithm. Section 3 describes the workflow, and the last section presents the results. The paper ends with a discussion and conclusion.

2 Background information

2.1 Geology

Located in southern France, this $700\mathrm{km}^2$ sedimentary basin is limited by the foothills of the Pyrenees to the south and west, the Corbières massif to the north and the Mediterranean Sea to the east (Fig. 1). This basin originates from the opening of the Gulf of Lion (Oligocene to Miocene) before being largely eroded by the Messinian Salinity Crisis (MSC) (Clauzon et al., 2015). It is with the drying up of the Mediterranean Sea that the Miocene was exposed and eroded, approximately 6 My ago (Lofi et al., 2005). During the Pliocene, the basin was filled up again, with Gilbert delta reworking the sediments generated by the sub-aerial Messinian unconformity. The sediments grade to wave-dominated deltas (Sandy Marine Pliocene or PMS) to fluvial dominated delta with the continental part corresponding to the Continental Pliocene (PC). On top of the stratigraphic pile, Quaternary sediments associated with rivers and lagoon systems have been deposited.

https://doi.org/10.5194/hess-2020-96
Preprint. Discussion started: 14 May 2020

Hydrology and Earth System Sciences
Discussions
Open Access
EGU

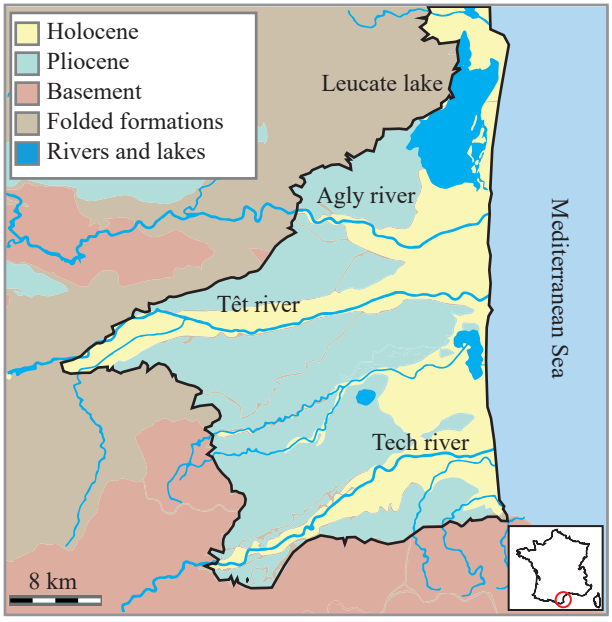

Figure 1. Simplified geological map of the Roussillon Plio-Quaternary aquifer.

The Pliocene layer is composed of different sandstone units separated by silt and clay layers of low permeability (Duvail, 2012; Aunay et al., 2006). The main source of sediments came from the weathering of the massifs surrounding the Roussillon's plain. Its depth increases towards the coastline, where its maximum thickness reaches 300 m (Duvail et al., 2005).

Based on field observations, the PC can be considered as a classical fluvial system. Near the relief, the association of high energy systems and the large amount of available sediments created alluvial fan deposits, composed of sandstone conglomerates. These alluvial fans have an extend of 1-3km radius and can be more than 10m thick. Fans merge together producing larger bodies of 3 to 6km wide and over 60m thick. The alluvial fans rapidly evolve to braided river deposits composed of coarse sands and sandstone conglomerates. These braided structures have generally an extend of 100-150m width and are 1-5m thick. It appears that these networks can be laterally and vertically well connected, forming very dense and wide objects near their sources. With the decrease of the sedimentary slope, the structures tend to evolve to meander rivers. Their deposits are still relatively coarse, yet much more sorted, and well contained within a single channel, their width reaches up to 300m and their thickness up to 12m. The connectivity of the river bed deposits is hard to observe either in the vertical or in the horizontal directions. Three other sedimentary elements are also intrinsically developed within the alluvial plain. The first two are the crevasse splay deposits and the levees, which are both directly related to the river's banks flooding dynamic. The last element is the plain itself characterized by a fine grained (silt to shale) sedimentation corresponding to the decanting process of flooding events.

https://doi.org/10.5194/hess-2020-96
Preprint. Discussion started: 14 May 2020


Hydrology and Earth System Sciences
Discussions

2.2 Hydrogeology

From a hydrogeological perspective, the study area contains two main aquifers; the Quaternary located in the shallow alluvial deposits along the rivers (Agly, Têt and Tech), and the Continental and Marine Pliocene aquifer located deeper and covering the whole basin (Fig. 1). These aquifers are exploited for agriculture and domestic use.

Due to its large extend, both onshore and offshore, the Pliocene's aquifer represents a large water reservoir. However, due to uncertainties related to its properties and recharge processes, the management of this resource is difficult. In the 1960s, the piezometric level in the PC was artesian in some locations and up to 8m higher on average as compared to the 2012 data. In recent years and close to the seashore, this exploitation has lowered the groundwater level below sea level during the summer months, when withdrawals are most intense. This situation raises concerns about seawater intrusion risk on the coastal part of the Pliocene aquifer.

As a consequence of climate change, groundwater reserves and recharge may decrease in the near future. For a scenario where the average annual temperature increases of 1.5C°associated with a decrease in precipitation rate, rivers flow could drop by 40% over the next 30 years (Chauveau et al., 2013), which will automatically create new stress on the groundwater resource. Considering that the multi-layer Plio-Quaternary Roussillon's aquifer accounts for almost 80% of the resources used for drinking waters, there is an urgent need to understand its behavior in order to manage this resource in a sustainable manner to face global change impacts (Caballero and Ladouche, 2015).

2.3 Multiple-point statistics and DeeSse

The essential ingredient of MPS techniques is the TI. The TI is a conceptual model displaying the structures the user wants to simulate. The use of TI gives flexibility and creativity to the modeller. Unlike some other geostatistical methods such as variogram, utilization of training image allows specialists from different fields to discuss together about the geometry and the type of heterogeneity of a model.

A TI can either be stationary or non-stationary. Stationary TIs are easier to use, they display a repetition of patterns with a homogeneous spatial distribution, *i.e.* the same type of spatial features is present everywhere in the grid. On the opposite, non-stationary TIs, displaying different kinds of structures depending on the location, they generally include more information and are more complex. When working with non-stationary TI, some rules must be observed in order to produce realistic simulations. Since the repetition of patterns is not homogeneous on such TI, one or several auxiliary variables are required to describe patterns spatial distribution. In the simulation grid, corresponding auxiliary variables are defined to control the spatial location of the structures that have to be simulated (Chugunova and Hu, 2008). With this information, patterns are not mixed together when simulated and trend characteristics can be reproduced. Auxiliary variable for the simulation grid are often called trend maps, because they allow to control the trend of the simulated structures.

A rotation map can also be used to orientate differently the patterns in the simulation grid compared to their orientation in the TI. Hence, the specific spatial features displayed in the TI can follow the same orientation everywhere, which facilitates the construction of the conceptual model, whereas the rotation map is used to define the local orientation in the simulation grid.

https://doi.org/10.5194/hess-2020-96
Preprint. Discussion started: 14 May 2020


Hydrology and Earth System Sciences
Discussions

Such map consists of angle values defined on the simulation grid: at each pixel, the given angle specifies a rotation that must be applied to the TI structures.

The DeeSse code is used in this project, which is an implementation of the direct sampling method (Mariethoz et al., 2010). The algorithm is controlled by three main parameters, e.g. n- number of neighboring nodes, f-scan fraction, t-distance threshold. The first one, n, defines the maximum number of nodes considered when comparing a pattern in the TI and in the simulation grid. At the beginning of the simulation, these n closest points are likely to be located far away from the simulated point. However, as the simulation progresses, the density of simulated point increases and the n closest points are located near the central point. This feature enables DeeSse to reproduce structures of all sizes during the simulation, starting with large ones and finishing with small and fine structures (Mariethoz et al., 2010). The second parameter is the threshold value t. When comparing patterns during the simulation, DeeSse calculates the pattern similarity between the TI and the simulation grid with a distance value. A perfect match between the patterns represents a distance of 0 and completely different patterns correspond to a distance of 1. If the distance calculated at the first random position in the TI is larger than the threshold, another point is chosen randomly in the TI and the distance is re-calculated. This is repeated until the value of the distance has reached the threshold or if a perfect match is found, then DeeSse copies the value of the central point found in the TI into the simulation grid. The last parameter, f, allows to limit the simulation time while conserving realistic patterns reproduction. If a fraction f of the TI is scanned without finding a pattern satisfying the threshold condition t, then the best node scanned so far (corresponding to the minimal distance between patterns) is retrieved. The same principles are used for categorical and continuous variables with an adapted definition of the distance. For multivariate simulation, one pattern per variable is considered, with the same central node, and one threshold value per variable.

3 Materials and Methods

This section presents the different elements that constitute the proposed MPS workflow. The elements are presented in their chronological order. The section starts by an overview of the workflow before describing the different steps more in details.

3.1 Overview

The first step of the workflow consists in interpreting the geophysical logs and geological field observations to establish the geological concept and build the hard conditioning data set.

The second step consists of converting these observations and concepts into one or several training images. This step is an iterative task, the modeller works with the geologist and they come up with one or several representative TI(s) of the system.

Here, the TI used for the PC layer, is a 2D non-stationary TI composed of 6 sedimentary facies. The TI imposes constraints regarding the geometry of the simulation grid and on the auxiliary information that have to be incorporated in the model. Regarding the PC layer, the simulation grid is created based on the bottom topography of the PC, in a flattened space, where 2D simulations can be generated in layers sharing the same age of deposition.

https://doi.org/10.5194/hess-2020-96
Preprint. Discussion started: 14 May 2020


Hydrology and Earth System Sciences
Discussions

In order to cope with the non-stationary TI, we use two auxiliary variable maps, one for the TI and one for the simulation grid. For the TI, the auxiliary variable is simply the x coordinate that is re-scaled between 0 and 1, this variable will inform the algorithm on the patterns location in the TI. For the simulation grid, we compute the auxiliary variable by solving numerically a diffusivity equation with proper boundary conditions allowing to mimic the general trend of sediment transport from the sediment source, on the west of the basin, to the coast. The last element that is incorporated in the model is rotation maps. The use of the direct sampling algorithm allows us to work with continuous rotation maps, defined through all the nodes of the grid (Mariethoz et al., 2010), whereas classic MPS techniques require to define rotation zones of unique value (de Carvalho et al., 2017). In addition, two continuous rotation maps are used to define the rotation bounds for the simulation with a tolerance of $\pm 10°$ on the rotation values. Theses rotation maps are obtained by kriging data that constrain the paleo-orientations of the main paleo-rivers.

The 3D model is then composed of stacked 2D simulations constrained by 3D auxiliary information. It appears that the creation of a 3D TI would have been too complex in regard of the available knowledge of the facies that compose the plain. To compensate for this choice and to take most of the information of the hard data set, the 3D grid is created with a rather fine resolution along the z axis ($2m$), which corresponds to the smallest body's dimension encountered in the plain. The vertical transition between facies is controlled by simulating additional conditioning data points between two 2D simulations. The values assigned to these sampled points are based on the vertical transition distribution of the facies, inferred from the hard data set. This process allows to bypass the creation of a 3D TI and to simulate in 2D with objects of a realistic z dimension.

The last step consists in generating a set of simulations to characterize the uncertainties. Probability and entropy maps are computed to summarize this information.

3.2 Hard data set

Hard data correspond to field observations assigned to cell values in the simulation grid. The hard conditioning data set of the PC model is composed of 52 well logs (gamma-ray and resistivity logs), which have been described and interpreted in term of electrofacies. The boreholes are not homogeneously distributed on the plain, but are mainly located along the Têt river and in the central zone of the Roussillon's plain.

The gamma ray and resistivity logs allowed to identify changes in sedimentary deposits and grain distribution along depth. Sand sediments have a small gamma ray response producing small peaks on the curve, whereas clay sediments produce high response peaks due to their high content in radioactive elements (Serra et al., 1975). By studying the evolution of these response curves, the sedimentary facies can be identified and assigned at a certain depth. A complete description of the interpretation process for the electrofacies of the PC layer can be found in Duvail (2008).

As presented in the geology section 2.1, six facies are identified in the outcrops; alluvial fan, braided river, meander river, crevasse splay, levee and floodplain deposits. Due to the small size of the levee deposit, its identification on the logs is not possible and would lead to misinterpretations. Therefore, only 5 out of the 6 facies are interpreted in the well logs.

https://doi.org/10.5194/hess-2020-96
Preprint. Discussion started: 14 May 2020


Hydrology and Earth System Sciences
Discussions

The hard conditioning data set also incorporates geological information from the geological map of the Roussillon. These data correspond to the mapped PC alluvial fan outcrop and are associated to the alluvial fan facies. It is essential to condition the model to the geological map where the simulated layers are exposed.

The final conditioning set results of 3500 interpreted points, that are being used during the simulation as hard conditioning data.

3.3 Training Images

Based on field observations, well logs analysis and the general understanding of the sedimentary processes composing the PC, three TIs, corresponding to different possible conceptual representations of the PC, are created and tested in 2D simulations (Fig. 2). As discussed by Høyer et al. (2017), the creation of the TI is an iterative task and it is always preferable to compare TIs not only on their structural aspects but also on the MPS simulation outputs. The first TI (Fig. 2a) is created based on a conceptual interpretation of an analogue river system from northern Italy where levees are not represented. The output of the 2D MPS simulation using this first TI resulted in the creation of a too large number of small braided/meander river deposits on the plain. Moreover, the alluvial fan facies is not simulated correctly, cutting heavily through braided river in the north-west part of the plain. The second TI (Fig. 2b) is created based on a more conventional conceptual representation of braided/meander system. It presents more complex braided structures and larger meander objects. The simulation output is composed of wider meander river deposits compare to what is observed in the outcrops. Moreover, the alluvial fan deposits -dark blue facies- are under-simulated compared to the observed alluvial fan deposits. Finally, we construct a third conceptual model of TI (Fig. 2c), which was constructed by trial and error adjustments. This TI is composed of six sedimentary facies and displays the evolution of an alluvial system from the mountain (sediment source) to the seashore, without including the estuary part (Nichols and Fisher, 2007) (Fig. 2d). In this last TI, meander channels have a straight shape due to the fact that this training image is not a snapshot of a fluvial system but rather an integrated view of a sedimentary system through time. This concept is illustrated in Fig. 2e, with the meander river facies used as an example. At $t = 0$, the meander bed follows one path, controlled by the sedimentary slope and the topography. At $t = 1$ the meander river would have laterally migrated, which could cut through the previous one. Finally, at $t = 2$ it is possible to define an area of high river bed occurrences, where all the meander river bed facies would be located.The last one, $t = 3$, highlights the only possible location where crevasse splay and levee can be preserved, on the borders of the river bed. It is this TI that is used for the next modelling part of the workflow.

The final TI is composed of 100×125 cells with a $100 \times 100m$ dimension. These dimensions are chosen in order to avoid any affinity transformation during the simulation. To propose some variability and not over control the transition distance between braided and meander deposits, the final TI laterally reproduces different fluvial systems (Fig. 2c). The dimension of the crevasse splay deposit increases with the decrease of the sedimentary slope (assuming the sedimentary slope decreases as we move from the sediment sources to the seashore). Finally, the levee facies is incorporated in the TI outside of the meander bed objects. Even if this facies is not described in the boreholes data, its spatial location will be constrained by the meander facies during simulation.

https://doi.org/10.5194/hess-2020-96
Preprint. Discussion started: 14 May 2020

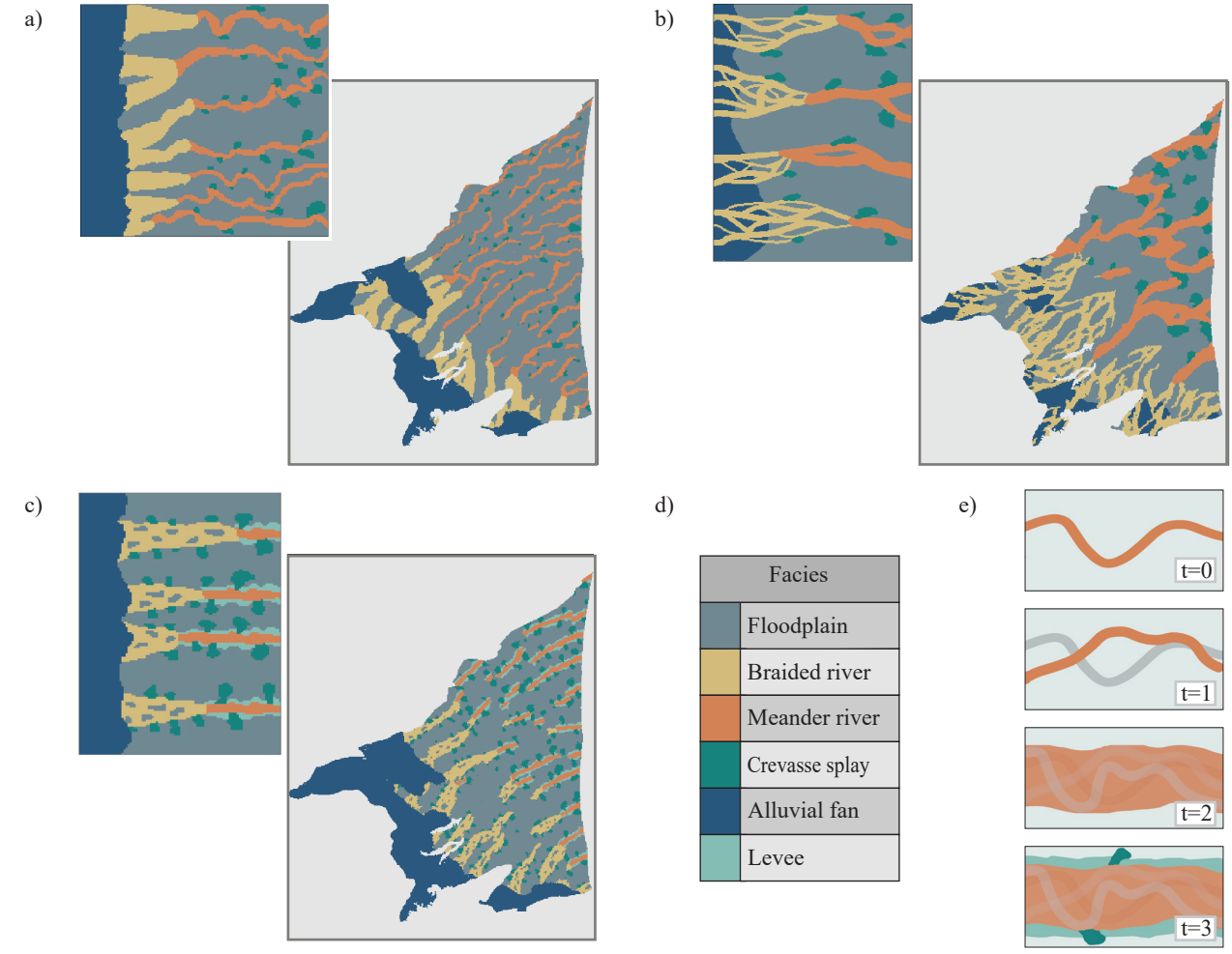

Figure 2. TIs associated with their corresponding 2D MPS simulations. a) an Italian analogue TI, b) a conceptual analogue TI and c) a TI created based on outcrop description and general knowledge of the Roussillon's plain. d) the six sedimentary facies of the TI. d) sedimentological concept of the TI.

3.4 Flattened space simulation grid

With the creation of the TI, the conceptual sedimentation process of the Roussillon's plain is now transferred into the model. The next step consists of creating a suitable simulation grid (SG) for the MPS simulation in accordance with the sedimentation process express by the TI. It is thus decided to create the 3D model by staking 2D simulations in a transformed grid.

A regular cartesian grid is used for the simulation with the following dimensions: $407 \times 504 \times 125$ cells ($25'641'000$ cells in total) with a cell dimension of $100 \times 100 \times 2m$. The z-axis dimension is defined in order to represent the minimal size of the

https://doi.org/10.5194/hess-2020-96
Preprint. Discussion started: 14 May 2020

Hydrology and Earth System Sciences
Discussions
Open Access
EGU

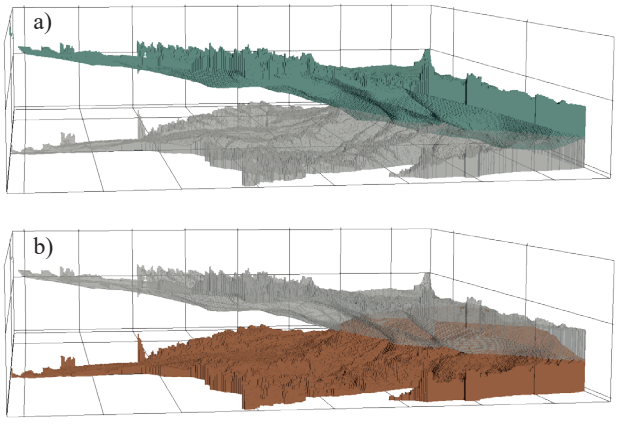

Figure 3. a) 3D grid of the PC layer (dark green). c) transformed grid (flattened space) of the PC layer inside which the 2D simulations are simulated (dark orange).

sedimentary objects that we want to model while the x and y cell dimensions are defined to optimize the resolution of the modelled objects while keeping the computing time reasonable.

Digital elevation maps corresponding to the top and bottom altitudes of the PC layer (Duvail, 2012) are used to select the active cells of the 3D simulation grid, the final volume of the PC layer is composed of $3'753'230$ active cells (Fig. 3a). Since the TI represents the sedimentary evolution of a fluvial system, the 2D simulations have to be carried out in cells that share the same age of deposition. This requires to transform our 3D grid based on the topography of the bottom layer of the PC (Fig. 3b). A vertical shift is applied to each column of cells to flatten the base of the grid to the bottom of the Pliocene. With this transformation (flattened space), we create a 3D grid where it is possible to simulate inside horizontal layer z_i composed of cells sharing approximately the same age of deposition.

3.5 Trend Maps

In order to cope with the non-stationary TI, the model has to be constrained with one auxiliary variable map (trend map) for the TI and one for the simulation grid. For the TI, the trend map is simply the x coordinate re-scaled between 0 and 1 and corresponds to the lateral evolution of the fluvial system. This trend has to be associated with a trend map of similar range for the simulation grid.

Creating a trend map for the 3D simulation grid is complex due to the geometry of the 2D layers and therefore requires to develop a new approach, different from the one used for the TI. In the flattened space simulation grid, the auxiliary variable is computed by solving numerically a diffusivity equation with proper boundary conditions in the 2D grid. This problem is similar to the simulation of the hydraulic head in a homogeneous confined aquifer for a steady state flow. We associate the evolution of the hydraulic head between source zones (river input zones) and an outflow zone (the sea shore) and consider

https://doi.org/10.5194/hess-2020-96
Preprint. Discussion started: 14 May 2020

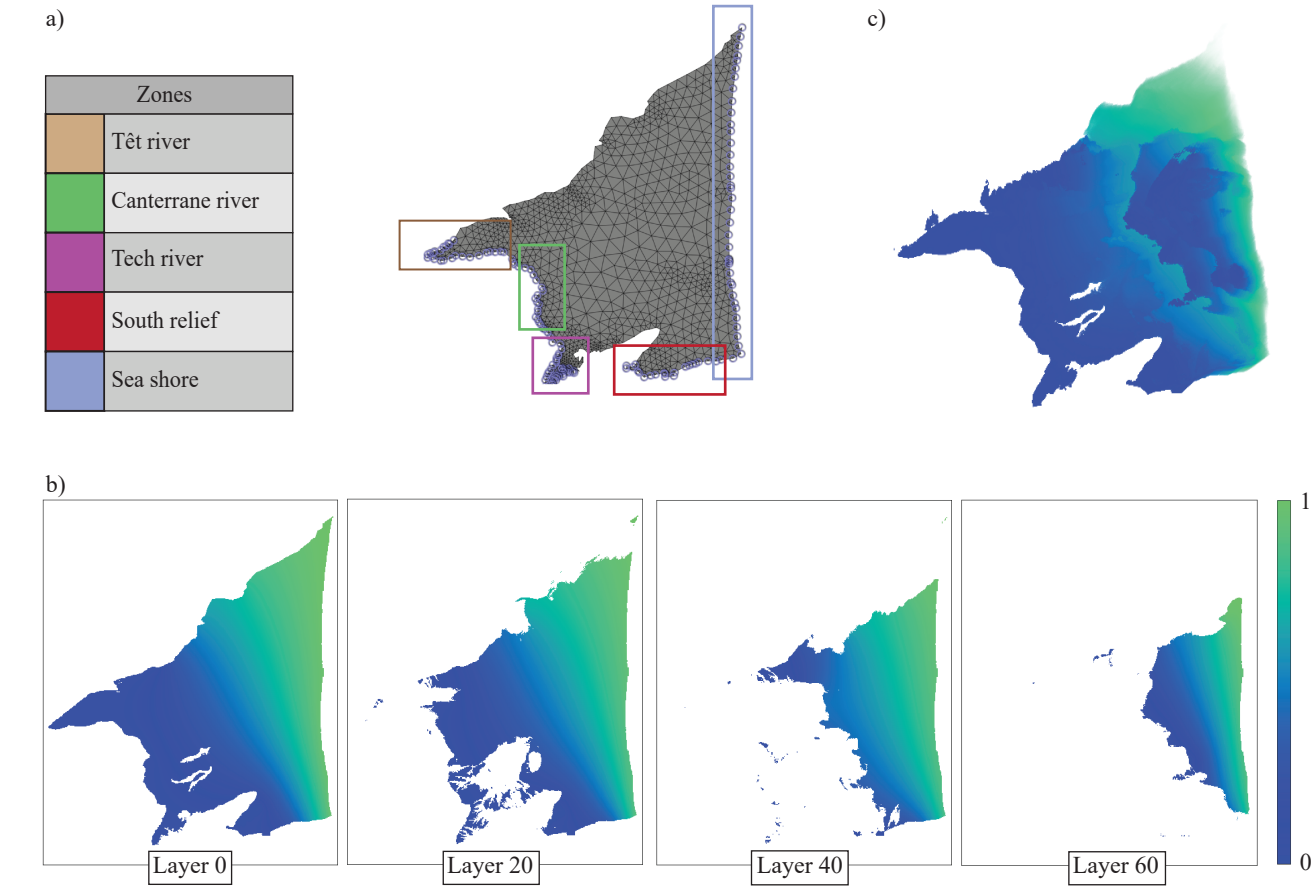

Figure 4. a) meshed grid with the four input zones and the one output zone used for the resolution of the diffusivity equation, b) different 2D layers that compose the 3D trend map of the transformed grid, c) top view of the 3D (transformed/flattened) trend map, where the progradation of the trend value towards the sea shore is visible. Both vertical and lateral trends of the PC are integrated to the 3D trend map.

the result of the diffusivity equation (taking values between $[0, 1]$) as a proxy for describing the evolution of the sedimentary system in the SG (Fig. 4a). The four input zones correspond to the three main paleo-rivers entrances and to the south relief zone where alluvial fan deposits are known to be present (Fig. 4a). The output zone corresponds to the seashore.

This approach is also applied to create the vertical sedimentation trend of the plain, corresponding to the progradation of the sedimentary system towards the sea. By simulating 12 different representative 2D trend layers (Fig. 4 b) and combining them together vertically (assigning the first trend layer to the layers 0-9, the second trend layer to the layers 10-19 and so on), a complex 3D trend map is obtained. This trend map accounts for both vertical and lateral sedimentation trends that characterize the Roussillon's plain (Fig. 4c).

https://doi.org/10.5194/hess-2020-96
Preprint. Discussion started: 14 May 2020

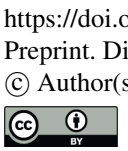

Hydrology and Earth System Sciences
Discussions
Open Access
EGU

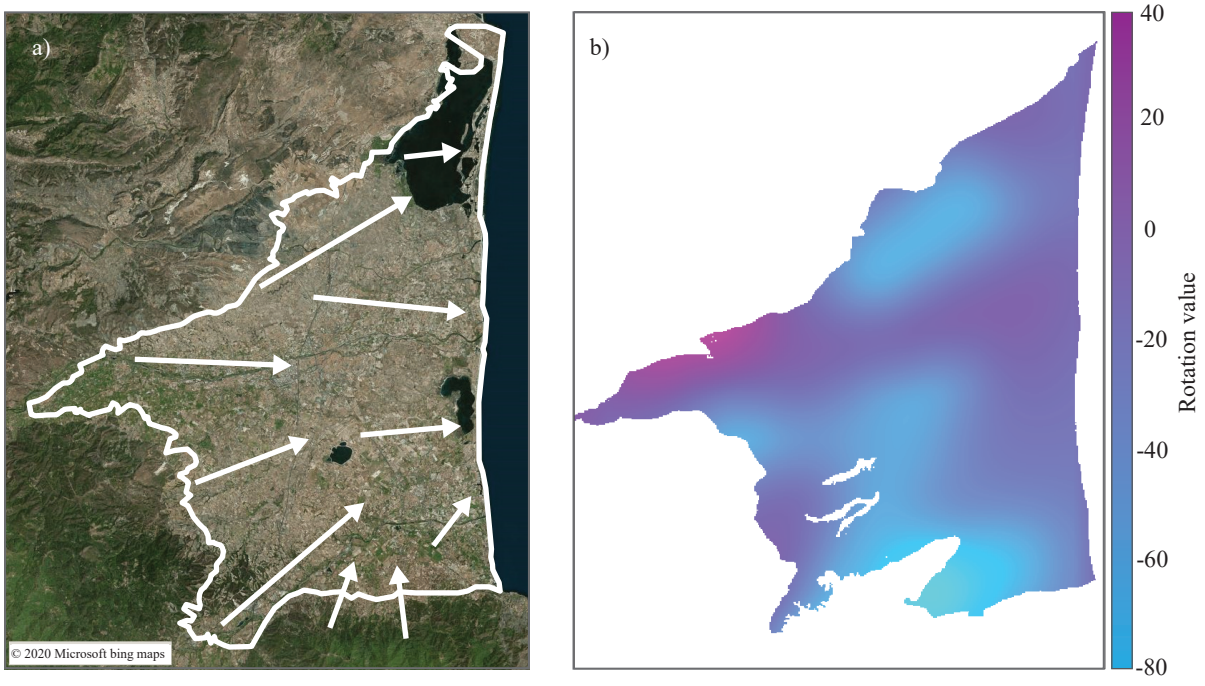

Figure 5. a) interpreted orientation of the paleo river in the Roussillon's plain, b) interpolated continuous kriged values, where a positive rotation value corresponds to a clock-wise pattern rotation and and a negative rotation value corresponds to a anti-clock-wise pattern rotation.

3.6 Rotation Maps

A 2D rotation map is created to control the orientation of the structures in the SG, relative to their orientations in the TI. This map is built based on data gathered from field observations and interpretations of assumed rivers' paleo-orientations (Fig. 5a). The main river influx came from the Têt river in the central part of the basin and from the Tech river in the south-west part. Based on these orientations, a fictive rotation point set is created and interpolated using kriging.

The orientation map is based on interpretation and therefore uncertain. DeeSse allows to account for this uncertainty. A tolerance of +/- 10° is considered and added/subtracted to the kriged map to obtain two rotation maps: one with the minimal angle values and one with the maximal angle values.

The 3D maps are then created by extruding these rotation values along the z-axis, assuming that the variation of the paleo-orientations through time is encompassed within the tolerance values.

3.7 Vertical transition

To control the vertical transition from one layer to the next one, we developed a simple sampling approach, illustrated in Fig. 6. The approach starts by simulating the first layer of the transformed grid (layer 0/bottom layer) using only the borehole hard data set as conditioning data. Once this layer is simulated, points are sampled from this simulated layer and propagated as

https://doi.org/10.5194/hess-2020-96
Preprint. Discussion started: 14 May 2020


Hydrology and Earth System Sciences
Discussions

additional (or secondary) hard data for the next layer. The facies value assigned to these points is drawn accordingly to the vertical transition probability between two facies, calculated from the boreholes hard data set.

Three parameters control this method, the first one defines which facies have to be sampled. By default, all the facies can be sampled. However, after some tests, it appeared that for the Roussillon case, the best way to control the vertical continuity was to sample only from three facies: the alluvial fan, the braided river and the meander river facies. The second parameter is the sampling rate, it was fixed by trial and error at 1% of the number of simulated cells for each of the 3 facies. The last parameter controls the maximum number of successive layers that are simulated using the sampling approach. This mechanism allows to control indirectly the maximal vertical size of the objects. This parameter was set to 6 for the Roussillon case, meaning that after six successive layers simulated using the approach, the next simulated layer will not use secondary sampled hard data.

Without this approach the vertical transition between facies would only be controlled by the hard conditioning data which are scarce compared to the size of the SG.

3.8 DeeSse parameters

The main parameters used for the MPS simulation with DeeSse were tested and chosen in order to minimize the simulation time without impairing the quality of the outputs. Two variables are considered: the facies (categorical) and the trend (continuous). The parameters defined for these two properties are the search ellipsoid which allows to limit the size of the pattern, the maximal number of pattern nodes (n) and the acceptance threshold (t).

The search ellipsoids are identical for both variables and are defined by a radius of 20 cells in x and y axis directions and 0 along z because 2D simulations are performed. The maximal number of nodes is set to $n = 24$ for the facies variable and set to $n = 5$ nodes for the trend variable. The larger number of neighboring nodes for the facies is defined to ensure a proper pattern reproduction during the simulation at both large and fine scales. Since the trend variable is defined for every node of the SG, there is no need to define a large number of pattern nodes for that property. The threshold t that controls the pattern quality reproduction is set to 0.05 for the facies property and to 0.25 for the trend property. Finally, the maximal scanned fraction (f) of the TI is set to 0.75.

Once satisfied with the 3D simulation output, the last step of the approach consists of producing a large number of simulations in order to compare them and to study the uncertainty of the model. The simulations are run on a CPU cluster, allowing to parallelize the computational load between different CPUs.

4 Simulation results

The following section presents the results of the workflow and the models obtained with DeeSse. The general aspect of the simulation is first discussed, before focusing on the ensemble statistics results calculated from 50 simulations sets.

Note that MPS validation is still an active research topic. Some tests and approaches are discussed for example by Mariethoz and Caers (2014). Due to the small number of hard conditioning data, we limit ourselves in this work to analyse the plausibility

https://doi.org/10.5194/hess-2020-96
Preprint. Discussion started: 14 May 2020

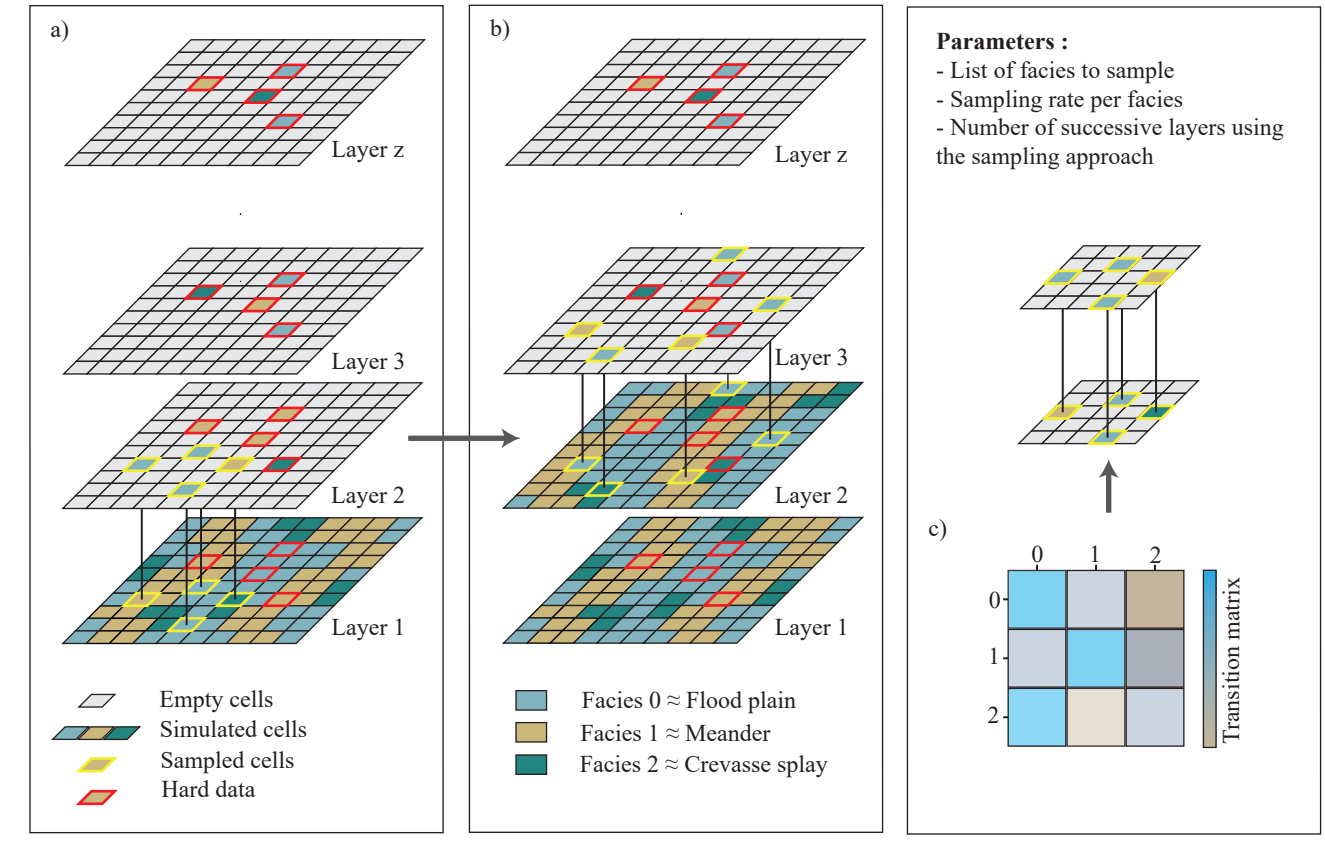

Figure 6. a) the first simulation takes place with only the hard data set as conditioning data. Then, a set of cells is sampled (in yellow) and used as new conditioning data for the next simulation. b) the process is repeated until the defined number of successive layers is reached. Once reached a simulation takes place without a sampling set. c) the value of the sampled cell is drawn based on the vertical transition matrix, calculated from the borehole data set.

of the geological patterns in the simulations with respect to the conceptual model, the final geological uncertainty resulting from the model, and some summary statistics.

4.1 3D simulation

One simulation is presented in Fig. 7. The first observation is that the model reproduces well the training image patterns over the different layers of the grid. All the main features of the TI are well reproduced and not too disconnected as it can be observed in the different horizontal-sections (Fig 7c) . Some discontinuities between the braided and meander deposits can be observed and are probably due to the presence of hard conditioning data, which doesn't match the pattern locations imposed by the SG trend maps. The continuous rotation maps produce smooth pattern rotations, which could not be obtained with classical zonal rotation. The use of continuous rotation maps helps to not break the pattern continuity and to create realistic simulations.

https://doi.org/10.5194/hess-2020-96
Preprint. Discussion started: 14 May 2020

Hydrology and Earth System Sciences
Discussions
Open Access
EGU

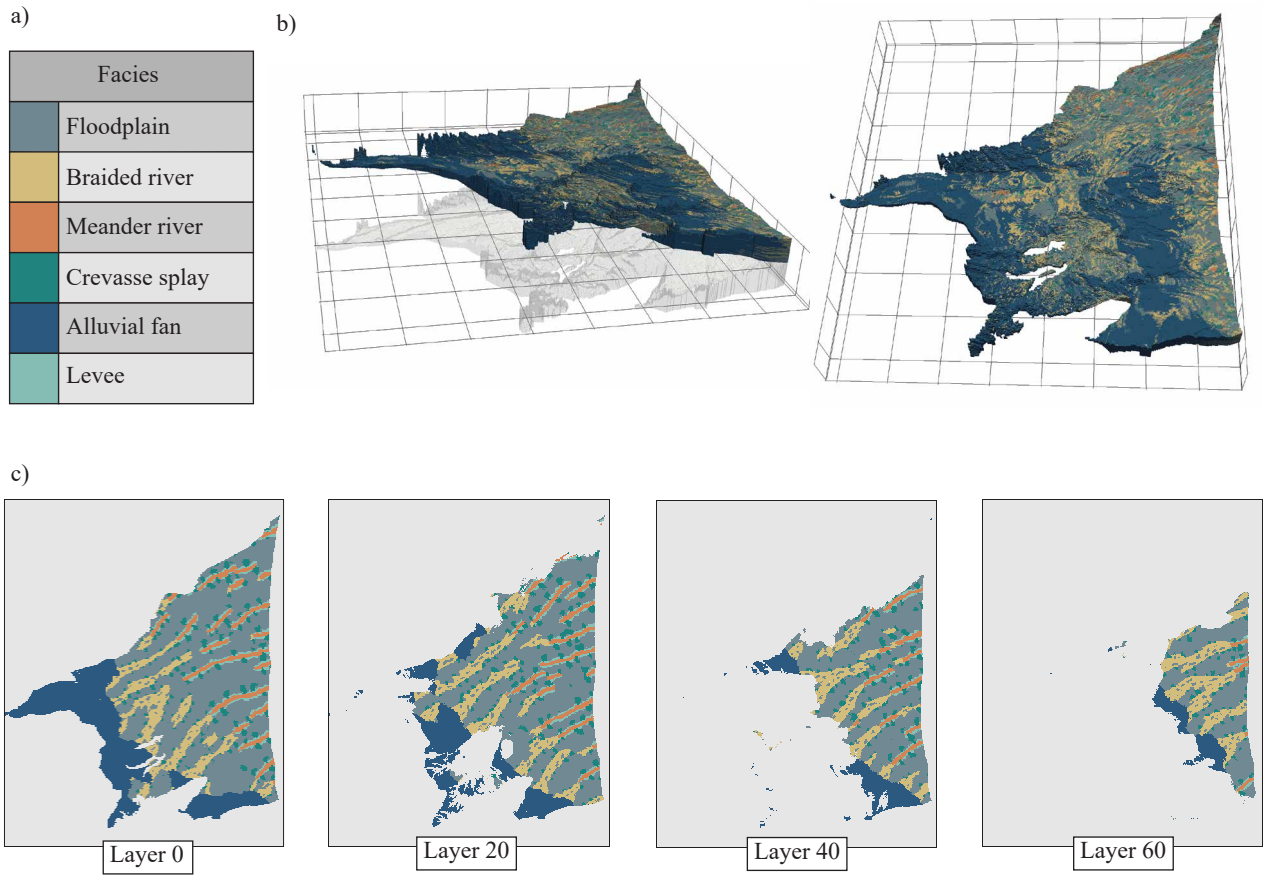

Figure 7. a) the 6 simulated facies, c) one 3D model of the simulations set, in the original 3D grid (left figure), and in the transformed grid (right figure). b) different z-layers (horizontal sections in the 3D transformed grid, where the 2D simulations are carried-on).

Regarding the non-stationarity, we can see in the 3D view (Fig. 7b) that the simulated structures successfully follow the trend imposed by the auxiliary variable. In particular, the progradation trend imposed to the grid succeeds to reproduce a realistic vertical progradation of the system. The alluvial fans, which represents the start of the sedimentary system, gradually move toward the sea as the depth decreases in the model.

One 3D model, composed of $3'753'230$ active cells, is generated in about 15min on a Intel®Core i7-7700 CPU at 3.6GHz.

4.2 Probability Maps

Simulating a large number of realizations enables us to calculate probability maps (Fig. 8) and the pixel wise entropy of the simulations set (Fig. 9).

https://doi.org/10.5194/hess-2020-96
Preprint. Discussion started: 14 May 2020


Hydrology and Earth System Sciences
Discussions

The probability maps display the probability of facies occurrence at each grid location based on 50 simulations (Fig. 8). If a facies is largely constrained at a spatial location, it is likely that all the simulations will simulate this facies at the same location and thus the probability map will display either very high or very low value at this spatial location. On the contrary, if a facies is less constrained, its probability map will display larger zones of occurrence through the simulations with more moderate values. The zones of extreme values are generally around hard conditioning data locations, which induce zones of low variability near them. These maps help the modeller to understand the model and the associated uncertainties.

In Fig. 8, we can see that every facies has a different variability behaviour through the ensemble of simulation. However, the facies variability is not influenced by the depth of the simulated layer, every facies displaying the same probability range at different depths.

The alluvial fan facies is the more constrained of all of the simulated facies. It is mainly due to its low spatial variability imposed by the trend maps. The second most constrained facies are the floodplain deposit. It is mainly constrained by the other 5 facies, which explains its low variability in simulation. These high values are also linked to the dominance in proportion of this facies. For the braided river facies, the spatial probability of occurrence evolves through the layer and is mainly constrained by the hard data, creating zones of high probability. Moreover, the location of these facies are mainly controlled by the trend value of the simulation grid. The same observation can be transposed for the meander river facies. Finally, the crevasse splay deposits are homogeneously distributed through the layers and the levee facies is only simulated near the meander river facies

These probability maps, show that trend map has a strong influence on the patterns lateral location. These maps also highlight the fact that the model is not over-constrained by either the TI or the HD and reflect the uncertainties lying in our conceptual model. Finally, this analyse of the simulations outputs is satisfying since it shows that the model respect the depositionnal concept expressed by the TI and the trend map.

4.3 Entropy Map

The six probability maps are used to calculate the information entropy. The Shannon Entropy was introduced in the theory of information developed by Shannon in the middle of the 20th century (Shannon, 1948) and represents the amount of information that is included within a probabilistic distribution. As proposed by Wellmann and Regenauer-lieb (2012), information entropy is an effective tool to visualize uncertainties in a spatial context. The main advantage of the entropy, is that it summaries the overall uncertainty contained in a probability distribution with a single number. The entropy is defined as:

$$H = -\sum_{i=1}^{n} p_i \log_n(p_i) \tag{1}$$

where n is the base of the logarithm corresponding to the number of categories (facies, 6 in our case) and p_i the probability of occurrence of the i-th category. The entropy is maximal and equal to 1 when all the outcomes have maximum uncertainty and is equal to 0 when there is a perfect certainty on the outcome.

The entropy map (Fig. 9) shows that there is little geological uncertainty in the upstream part of the plain where the alluvial fan dominate. Similarly, the uncertainty is rather small in the transition zone between braided and meander river. The entropy

https://doi.org/10.5194/hess-2020-96
Preprint. Discussion started: 14 May 2020

Hydrology and Earth System Sciences
Discussions

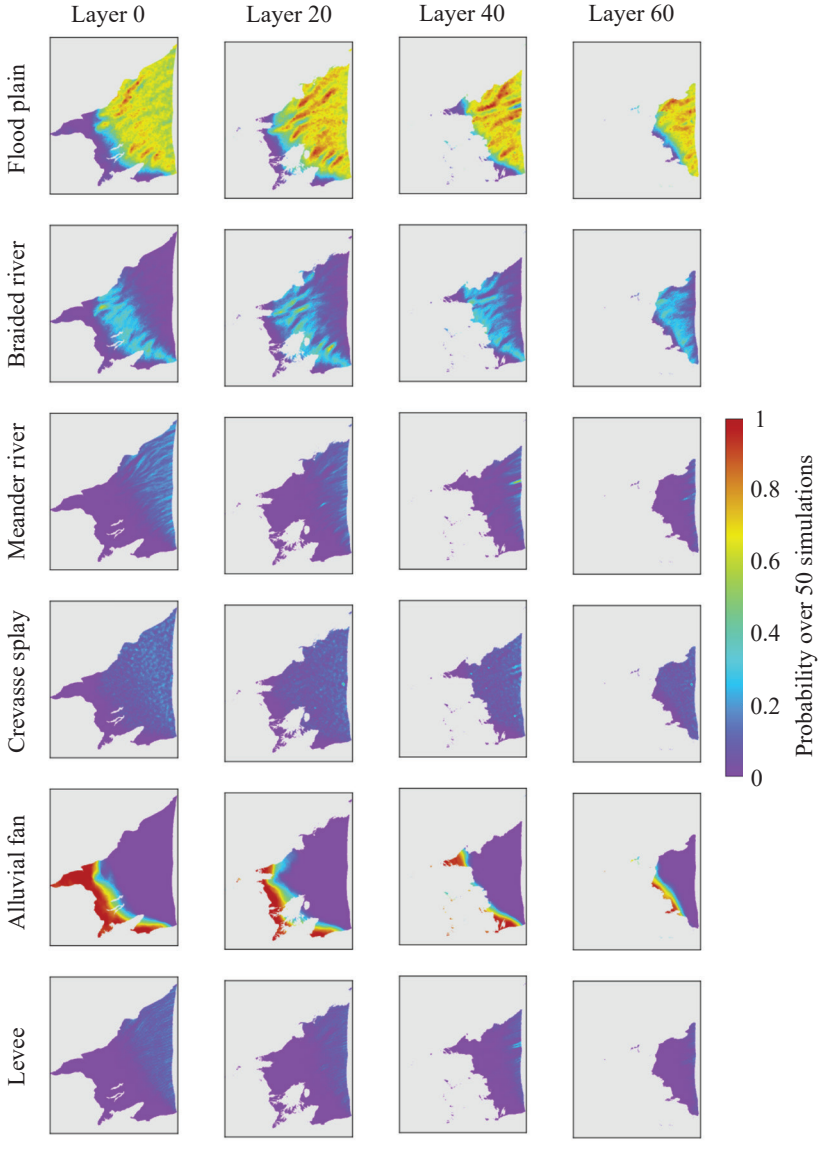

Figure 8. Probability maps of the 6 simulated facies at different depth. The probability maps are calculated over a 50 simulations set.

map also reveals that the meander river facies is mostly constrained by the hard data, limiting its possible spatial locations in the simulation grid.

4.4 Facies proportion and vertical transition

365 Figure 10a compares the proportion of facies of the TI, the hard conditioning data set and two sets containing 50 simulations each; the first one with the vertical sampling approach and the second without it. Overall, the proportion distributions of

https://doi.org/10.5194/hess-2020-96
Preprint. Discussion started: 14 May 2020

Hydrology and Earth System Sciences
Discussions

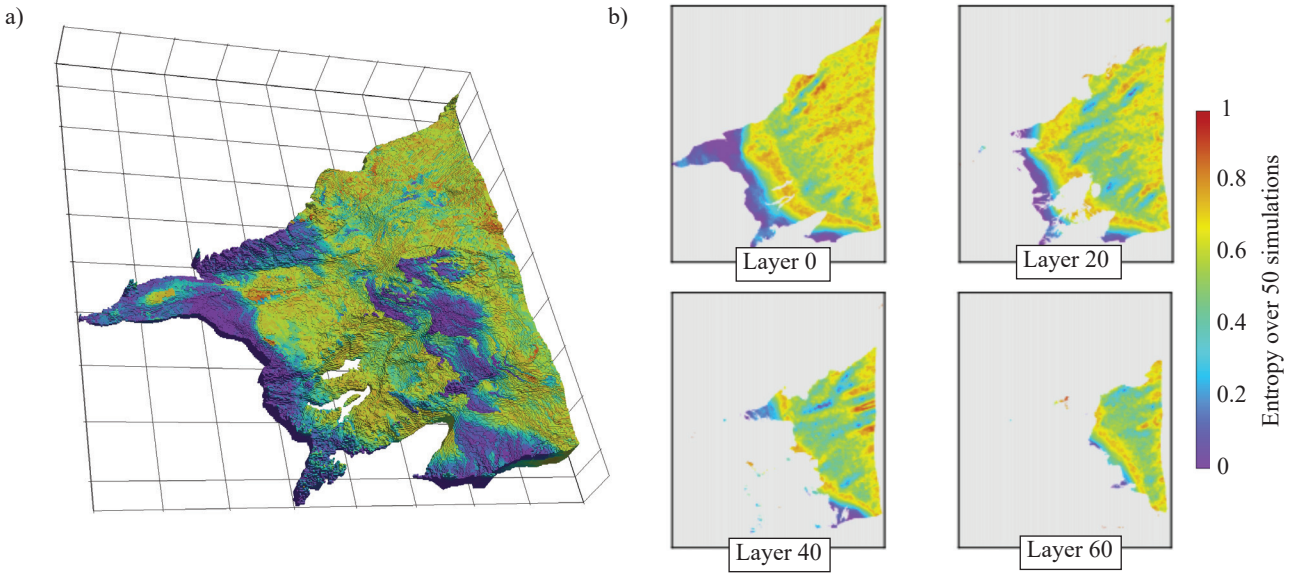

Figure 9. Shannon entropy of the model, calculated from the 6 facies probability maps. a) 3D views in the transformed grid, b) different horizontal 2D layers within the 3D transformed grid.

simulated facies is satisfying when we compare the simulation sets with the hard data. It appears that the proportions are controlled by both the TI and hard data proportions, with the hard data set having a slightly larger influence compare to the TI. This is reflected with the alluvial fan facies, which is less represented in the hard data set - mostly due to the central location on the plain of the majority of the boreholes - and less represented in the model compared to the TI proportion. This facies percentage distribution shows the importance of the hard data on the simulation and the consequence that can carry a biased hard data set.

To quantify the impact of the vertical sampling strategy on the simulations, we compare the vertical pixel-wise size distribution of the simulated object from the hard data set and the two simulation sets. To do so, a dissimilarity index is calculated for each simulated facies (Fig. 10b). This dissimilarity index quantifies the difference between two distributions, taking the vertical size distributions of the hard data set as the reference distributions (the closest to zero the dissimilarity value is, the more identical the distributions are). We use a normalized euclidean distance to calculate the index of dissimilarity. The alluvial fan facies is here not represented, because it is under-represented in the hard data set and a reference distribution cannot be inferred from it.

Overall, the simulation set using the vertical sampling strategy possesses distributions closer to the conditioning data (smaller dissimilarities value). The set using the vertical sampling strategy is composed of a larger number of thick objects as compared to the simulations set not using the sampling approach. Figure 10b shows the beneficial impact of the vertical sampling approach on the simulation outputs.

https://doi.org/10.5194/hess-2020-96
Preprint. Discussion started: 14 May 2020

Hydrology and Earth System Sciences
Discussions

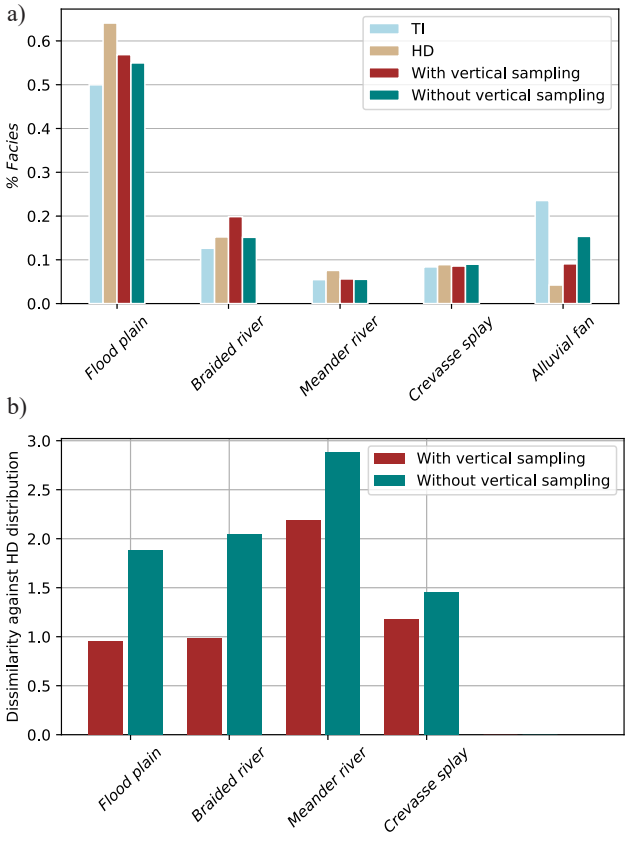

Figure 10. a) facies percentage in the training image, the hard data set, 3D simulation without vertical sampling and 3D simulation with vertical sampling. b) the dissimilarity values for the two simulation sets. The dissimilarity value is calculated against the vertical size distribution of the hard conditioning data.

5 Discussion and Conclusions

385 This study proposes a new workflow for the simulation of complex heterogeneous aquifer. Unlike more classical MPS studies, which rely on large primary or secondary hard data sets such as geophysics (Strebelle et al., 2002; Barfod et al., 2018; Høyer et al., 2017), this work relies on conceptual knowledge and auxiliary information.

The main novelties within this workflow are the use of 2D simulations accounting for trends computed by solving a diffusion equation, the use of two continuous maps of rotation angles to account for the uncertainty on the paleo-orientations, and the 390 transfer of conditioning data from layer to layer to constrain the vertical transitions between the facies.

The proposed approach is simpler and faster than one based on a 3D TI. It has the advantage of being more flexible during the development of the model, where all of the elements can be easily adapted to the specific case and tested. In particular, the

https://doi.org/10.5194/hess-2020-96
Preprint. Discussion started: 14 May 2020


Hydrology and Earth System Sciences
Discussions

possibility of using auxiliary information allows the modeller to approach each problem with a different angle making MPS, and especially DeeSse very flexible.

The study of the Roussillon plain shows the importance of testing different TIs to obtain acceptable structures. The TI must be created to reflect the general geological knowledge available for the study site and it must respect the interpreted data. One of the strengths of the MPS method is that it allows to test rapidly different concepts that can be discussed and adapted. Moreover, the use of complex auxiliary variable and continuous rotation maps allow the final model to account for that information while honoring the borehole data.

The robustness of the proposed methodology has been tested with two sets of 50 simulations, one set with the vertical sampling approach and the other one without it. Despite its relatively simple method, the vertical sampling improves the vertical object' size reproduction. The simulation without vertical sampling misses to create the large vertically connected objects, where the simulations with vertical sampling have a distribution more comparable to the hard data set distribution. These improvements, regarding the vertical objects size reproduction, are important, since the meander river deposits and the braided river deposits are known to have high aquifer potentials. Recreating the vertical connectivity of these objects is a key parameter for the future use of the geological model for the hydro-characterization of the aquifer.

The probability and the entropy maps show that the important sedimentary concepts have been well integrated into the model. The facies proportion distribution of the different objects is satisfactorily reproduced and is constrained by both the boreholes facies distribution and the TI distribution. The probability and the entropy maps also show a lack of hard data. Indeed, the hard data set used may not be fully representative of the facies distribution of the PC aquifer and the simulation can suffer from this bias. Regarding the vertical sampling approach, even if it improves the realism of the simulated object, the simulated shapes would benefit from additional constraints. The vertical transition matrix inferred from the boreholes can also present a bias due to their location or their non-representativeness of the real transition matrix.

Therefore, the model of the Roussillon plain would clearly benefit from additional boreholes with gamma ray and resistivity logs at locations that are not yet constrained. A denser data set would permit to conduct a meaningful cross validation exercise. At present, the data are not sufficient to really test carefully the predictive power of the MPS model. The model of the Roussillon plain would also benefit from additional information regarding the geometry of the sedimentological objects (their width, their lateral distribution...). Analogue data or geophysical inputs could help to better understand these geometries and could help in characterizing the transition zone between braided and meander river.

Finally, despite these possible improvements, this work demonstrates the applicability of DeeSse and the proposed workflow to simulate complex internal aquifer heterogeneity at a regional scale.

Code and data availability. The codes and data will be available soon on git hub : https://github.com/randlab/MPS_Roussillon.

https://doi.org/10.5194/hess-2020-96
Preprint. Discussion started: 14 May 2020

Hydrology and Earth System Sciences
Discussions
Open Access
EGU

Author contributions. V. Dall'Alba produced the different elements composing the model and the simulations and wrote the manuscript. C. Duvail and B. Issautier worked on the conceptual geological model and have supported the interpretation of the boreholes data set. J. Straubhaar and P. Renard contributed to the MPS simulations workflow. Y. Caballero supervised the project and contributed to the hydrogeology section of this paper. Finally, all of the authors reviewed the manuscript before submission.

Competing interests. The authors declare that they have no conflict of interest.

Acknowledgements. The authors thank the different partners of the Dem'Eaux Roussillon project and the University of Neuchâtel for supporting the development of this work.

https://doi.org/10.5194/hess-2020-96
Preprint. Discussion started: 14 May 2020

Hydrology and Earth System Sciences
Discussions

References

Aunay, B., Duvail, C., Giordana, G., Dörfliger, N., Le Strat, P., Montginoul, M., and Pistre, S.: A pluridisciplinary methodology for intregrated management of coastal aquifer - Geological, hydrogeological and economic studies of the Roussillon aquifer (Pyrénées-Orientales, France), VIE MILIEU, 56, 275–285, https://hal.archives-ouvertes.fr/hal-00453812/, 2006.

Barfod, A. A. S., Møller, I., Christiansen, A. V., Hoyer, A. S., Hoffimann, J., Straubhaar, J., and Caers, J.: Hydrostratigraphic modeling using multiple-point statistics and airborne transient electromagnetic methods, HYDROL EARTH SYST SC, 22, 3351–3373, https://doi.org/10.5194/hess-22-3351-2018, 2018.

Caballero, Y. and Ladouche, B.: Impact of climate change on groundwater in a confined Mediterranean aquifer, HYDROL EARTH SYST SC Discussions, 12, 10 109–10 156, https://doi.org/10.5194/hessd-12-10109-2015, 2015.

Chauveau, M., Chazot, S., Perrin, C., Bourgin, P.-Y., Sauquet, E., Vidal, J.-P., Rouchy, N., Martin, E., David, J., Norotte, T., Maugis, P., and De Lacaze, X.: Quels impacts des changements climatiques sur les eaux de surface en France à l'horizon 2070 ?, La Houille Blanche, 4, 5–15, https://doi.org/10.1051/lhb/2013027, 2013.

Chugunova, T. L. and Hu, L. Y.: Multiple-Point Simulations Constrained by Continuous Auxiliary Data, MATH GEOSCI, 40, 133–146, https://doi.org/10.1007/s11004-007-9142-4, 2008.

Clauzon, G., Le Strat, P., Duvail, C., Do Couto, D., Suc, J. P., Molliex, S., Bache, F., Besson, D., Lindsay, E. H., Opdyke, N. D., Rubino, J. L., Popescu, S. M., Haq, B. U., and Gorini, C.: The Roussillon Basin (S. France): A case-study to distinguish local and regional events between 6 and 3 Ma, MAR PETROL GEOL, 66, 18–40, https://doi.org/10.1016/j.marpetgeo.2015.03.012, 2015.

de Carvalho, P. R. M., da Costa, J. F. C. L., Rasera, L. G., and Varella, L. E. S.: Geostatistical facies simulation with geometric patterns of a petroleum reservoir, STOCH ENV RES RISK A, 31, 1805–1822, https://doi.org/10.1007/s00477-016-1243-5, 2017.

de Marsily, G., Delay, F., Gonçalvès, J., Renard, P., Teles, V., and Violette, S.: Dealing with spatial heterogeneity, HYDROGEOL J, 13, 161–183, https://doi.org/10.1007/s10040-004-0432-3, 2005.

Duvail, C.: Expression des facteurs régionaux et locaux dans l'enregistrement sédimentaire d'une marge passive. Exemple de la marge du Golfe du Lion, étudiée selon un continuum terre-mer, Thesis, Université de Montpellier 2, https://tel.archives-ouvertes.fr/tel-00438146, 2008.

Duvail, C.: Caractérisation de la géométrie et de l' architecture des formations du Pliocène de la plaine du Roussillon pour la modélisation hydrodynamique., Tech. rep., BRGM, Geoter, 2012.

Duvail, C., Gorini, C., Lofi, J., Le Strat, P., Clauzon, G., and dos Reis, A. T.: Correlation between onshore and offshore Pliocene-Quaternary systems tracts below the Roussillon Basin (eastern Pyrenees, France), MAR PETROL GEOL, 22, 747–756, https://doi.org/10.1016/j.marpetgeo.2005.03.009, 2005.

Høyer, A. S., Vignoli, G., Hansen, T. M., Vu, L. T., Keefer, D. A., and Jørgensen, F.: Multiple-point statistical simulation for hydrogeological models: 3-D training image development and conditioning strategies, HYDROL EARTH SYST SC, 21, 6069–6089, https://doi.org/10.5194/hess-21-6069-2017, 2017.

Hu, L. Y. and Chugunova, T.: Multiple-point geostatistics for modeling subsurface heterogeneity: A comprehensive review, WATER RESOUR RES, 44, 1–14, https://doi.org/10.1029/2008WR006993, 2008.

Journel, A. G.: Geostatistics for conditional simulation of ore bodies, ECON GEOL, 69, 673–687, https://doi.org/10.2113/gsecongeo.69.5.673, 1974.

https://doi.org/10.5194/hess-2020-96
Preprint. Discussion started: 14 May 2020

Lofi, J., Gorini, C., Berné, S., Clauzon, G., Dos Reis, A. T., Ryan, W. B. F., and Steckler, M. S.: Erosional processes and paleo-environmental changes in the Western Gulf of Lions (SW France) during the Messinian Salinity Crisis, MAR GEOL, 217, 1–30, https://doi.org/10.1016/j.margeo.2005.02.014, 2005.

Mariethoz, G. and Caers, J.: Multiple-Point Geostatistics: stochastic modeling with training images, Wiley-Blackwell. A John wiley and Sons, LTD, Publication, https://doi.org/10.1002/9781118662953, 2014.

Mariethoz, G., Renard, P., and Straubhaar, J.: The direct sampling method to perform multiple-point geostatistical simulations, WATER RESOUR RES, 46, 1–14, https://doi.org/10.1029/2008WR007621, 2010.

Matheron, G.: Principles of geostatistics, ECON GEOL, 58, 1246–1266, https://doi.org/10.2113/gsecongeo.58.8.1246, 1963.

Matheron, G., Beucher, H., De Fouquet, C., Galli, A., Guerillot, D., Ravenne, C., et al.: Conditional simulation of the geometry of fluvio-deltaic reservoirs, SOC PETROL ENG J, Spe annual technical conference and exhibition, https://doi.org/10.2118/16753-MS, 1987.

Naranjo-Fernández, N., Guardiola-Albert, C., and Montero-González, E.: Applying 3D geostatistical simulation to improve the groundwater management modelling of sedimentary aquifers: The case of Doñana (Southwest Spain), Water (Switzerland), 11, https://doi.org/10.3390/w11010039, 2018.

Nichols, G. J. and Fisher, J. A.: Processes, facies and architecture of fluvial distributary system deposits, SEDIMENT GEOL, 195, 75–90, https://doi.org/10.1016/j.sedgeo.2006.07.004, 2007.

Serra, O., Sulpice, L., et al.: Sedimentological analysis of shale-sand series from well logs, https://www.onepetro.org/conference-paper/SPWLA-1975-W, 1975.

Shannon, C. E.: A Mathematical Theory of Communication, BELL SYST TECH J, 5, 3, https://doi.org/10.1002/j.1538-7305.1948.tb01338.x, 1948.

Straubhaar, J.: DeeSse user's guide, Tech. rep., The Centre for Hydrogeology and Geothermics (CHYN), University of Neuchâtel: Neuchâtel, Switzerland, 2019.

Straubhaar, J., Renard, P., Mariethoz, G., Froidevaux, R., and Besson, O.: An improved parallel multiple-point algorithm using a list approach, MATH GEOSCI, 43, 305–328, https://doi.org/10.1007/s11004-011-9328-7, 2011.

Straubhaar, J., Walgenwitz, A., and Renard, P.: Parallel Multiple-Point Statistics Algorithm Based on List and Tree Structures, MATH GEOSCI, 45, 131–147, https://doi.org/10.1007/s11004-012-9437-y, 2013.

Strebelle, S., Payrazyan, K., and Caers, J.: Modeling of a Deepwater Turbidite Reservoir Conditional to Seismic Data Using Multiple-Point Geostatistics, SOC PETROL ENG Annual Technical Conference and Exhibition, https://doi.org/10.2118/77425-MS, 2002.

Tahmasebi, P., Hezarkhani, A., and Sahimi, M.: Multiple-point geostatistical modeling based on the cross-correlation functions, COMPUTAT GEOSCI, 16, 779–797, https://doi.org/10.1007/s10596-012-9287-1, 2012.

Wellmann, J. F. and Regenauer-lieb, K.: Tectonophysics Uncertainties have a meaning : Information entropy as a quality measure for 3-D geological models, TECTONOPHYSICS, 526-529, 207–216, https://doi.org/10.1016/j.tecto.2011.05.001, 2012.

Zhang, T., Switzer, P., and Journel, A.: Filter-based classification of training image patterns for spatial simulation, MATH GEOL, 38, 63–80, https://doi.org/10.1007/s11004-005-9004-x, 2006.